Let us suppose that $\hat{Q}_\omega$ is a constant, so representing a ''white-noise'' process in which all frequencies have the same amplitude.[2] The response of the SST anomalies that evolve, we assume, according to Eq. 12-1, is given by $T = \mathrm{Re}\,\hat{T}_\omega e^{i\omega t}$, where (see Problem 2 at end of chapter)

$$\hat{T}_\omega^2 = \left(\frac{\hat{Q}_\omega}{\gamma_O}\right)^2 \frac{1}{\omega^2 + \left(\frac{\lambda}{\gamma_O}\right)^2}. \qquad (12\text{-}2)$$

The T spectrum is plotted in Fig. 12.3a and has a very different character from that of the forcing. We see that $\omega_c = \lambda/\gamma_O$ defines a critical frequency that depends on the heat capacity of the ocean in contact with the atmosphere (set by h) and the strength of the air-sea coupling (set by λ). At frequencies $\omega > \omega_c$ the temperature response to white noise forcing decreases rapidly with frequency—the sloping straight line on the log-log plot. At frequencies $\omega < \omega_c$ the response levels out and becomes independent of ω as evident from the grey curve in Fig. 12.3a. For the parameters chosen above, $\omega_c = \frac{1}{300\ \mathrm{d}}$, and so one might expect SST variations with timescales much shorter than 300 d to be damped out, leaving variability only at timescales longer than this. This simple model (first studied by Hasselman, 1976), is the canonical example of how inertia introduced by slow elements of the climate system (in this case thermal inertia of the ocean's mixed layer) smooths out high frequencies to yield a slow response, a ''reddening'' of the spectrum of climate variability.

In comparison, Fig. 12.3b shows the observed temperature spectra of the atmosphere and of SST. Although the atmospheric spectrum is rather flat, the SST spectrum is much redder, somewhat consistent with the ω^{-2} dependence predicted by Eq. 12-2 above. Simple models of the type described here, explored further in Problem 2 at the end of the chapter, can be used to rationalize such observations.

One aspect of observed air-sea interaction in midlatitudes represented in the above model is that atmospheric changes tend to precede oceanic changes, strongly supporting the hypothesis that midlatitude year-to-year (and even decade-to-decade) variability primarily reflects the slow response of the ocean to forcing by atmospheric weather systems occurring on much shorter timescales. One might usefully call this kind of variability ''passive''—it involves modulation by ''slower'' components of the climate system (in this case the ocean) of random variability of the ''faster'' component (the atmosphere).

In tropical latitudes, however, changes in SST and tropical air temperatures and winds are more in phase with one another, reflecting the sensitivity of the tropical atmosphere to (moist) convection triggered from below. This sensitivity of the atmosphere to tropical SST can lead to ''active'' variability—coupled interactions between the atmosphere and the ocean in which changes in one system mutually reinforce changes in the other, resulting in an amplification. In the next section we discuss how such active coupling in the tropical Pacific manifests itself in a phenomenon of major climatic importance known as El Niño.

12.2. EL NIÑO AND THE SOUTHERN OSCILLATION

12.2.1. Interannual variability

Interannual variability of the atmosphere is particularly pronounced in the tropics, especially in the region of the Indian

[2] A spectrum, or part of a spectrum, which has less power at higher frequencies, is often called ''red,'' and one that has less power at lower frequencies, ''blue.'' A spectrum that has the same power at all frequencies is called ''white.'' These terms are widely used but imprecisely defined.

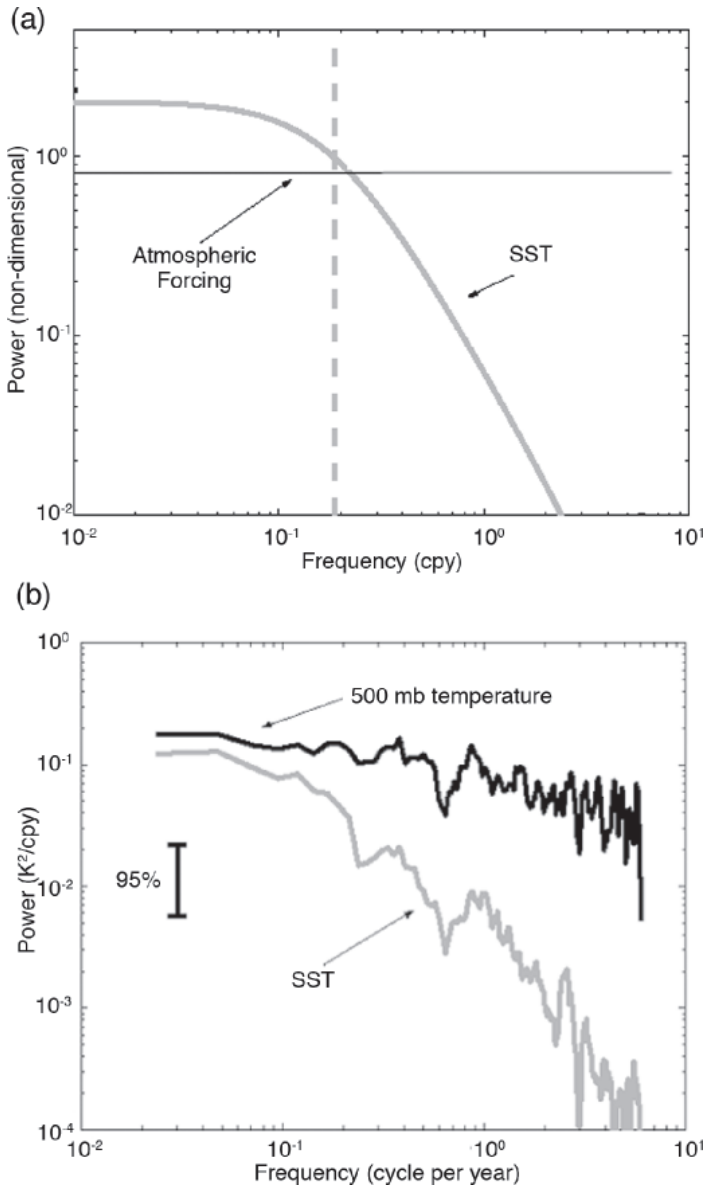

FIGURE 12.3. (a) The theoretical spectrum, Eq. 12-2, graphed on a log-log plot. The vertical grey dotted line indicates the frequency $\omega_c/2\pi$ where $\omega_c = \lambda/\gamma_O$ and is measured in cycles per year (cpy). For the parameters chosen in the text, $\omega_c = \frac{1}{300\text{ d}}$, and so the grey line is drawn at a frequency of $\frac{1}{2\pi}\frac{365\text{ d}}{300\text{ d}} = 0.19$ cpy. (b) Log-log plot of the power spectrum of atmospheric temperature at 500 mbar (black) and SST (grey) associated with the North Atlantic Oscillation, the leading mode of climate variability in the Atlantic sector. See Czaja et al (2003) for more details. The frequency is again expressed in cpy as in (a), and the power in K^2/cpy.

and Pacific Oceans, where it is evident, among other things, in occasional failures of the Indian monsoon, extensive droughts in Indonesia and much of Australia, and in unusual rainfall and wind patterns right across the equatorial Pacific Ocean as far as South America and extending beyond the tropics. This phenomenon has been known for a long time. For example, Charles Darwin, in *Voyage of the Beagle* (1831–1836), noted the tendency for climatic anomalies to occur simultaneously throughout the

tropics. Tropical climate variability was first comprehensively described in the 1920s by the meteorologist Gilbert Walker, who gave it the name *Southern Oscillation*.

Manifestations of interannual variability are not, however, confined to the atmosphere. The El Niño phenomenon has been known for centuries to the inhabitants of the equatorial coast of Peru. Until the middle of the 20th century, knowledge of this behavior was mostly confined to the coastal region, where an El Niño is manifested as unusual warmth of the (usually cold) surface waters in the far eastern equatorial Pacific (see Fig. 9.14), and is accompanied (for reasons to be discussed below) by poor fishing and unusual rains.[3] With the benefit of modern data coverage, it is clear that the oceanic El Niño and the atmospheric Southern Oscillation are manifestations of the same phenomenon, which is now widely known by the concatenated acronym ENSO. However, this was not always the case. It was not until the 1960s that Jacob Bjerknes[4] argued that the two phenomena are linked.

12.2.2. "Normal" conditions—equatorial upwelling and the Walker circulation

As discussed in Chapter 7, the lower tropical atmosphere is characterized by easterly trade winds, thus subjecting the tropical ocean to a westward wind stress (see, for example, Figs. 7.28b and 10.2). Let us begin by considering a hypothetical ocean on an Earth with no continents, and with a purely zonal, steady, wind stress $\tau < 0$ that is independent of longitude, acting on a two-layer ocean with a quiescent deep layer of density ρ_1, capped by a mixed layer of depth h and density $\rho_2 = \rho_1 - \Delta\rho$, as sketched in Fig. 12.4.

The dynamics of Ekman-driven upwelling and downwelling was discussed in Section 10.1. Here, near the equator, we must modify it slightly. As the equator is approached, the Coriolis parameter diminishes to zero and cannot be assumed to be constant. Instead we write $f = 2\Omega \sin\varphi \simeq \beta y$, where $y = a\varphi$ is the distance north of the equator, and $\beta = 2\Omega/a = 2.28 \times 10^{-11} \mathrm{m}^{-1}\,\mathrm{s}^{-1}$ is the equatorial value of the gradient of the Coriolis parameter. The steady zonal

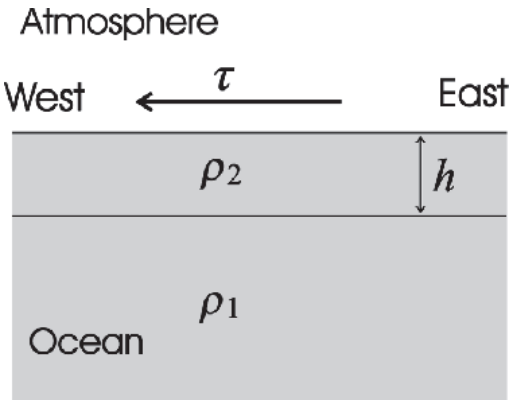

FIGURE 12.4. Schematic of a two-layer ocean model: the upper layer of depth h has a density ρ_2, which is less than the density of the lower layer, ρ_1. A wind stress τ blows over the upper layer.

[3] The name "El Niño"—the child (and, by implication, the Christ child)—stems from the observation of the annual onset of a warm current off the Peruvian coast around Christmas. El Niño originally referred to this seasonal warm current that appeared every year, but the term is now reserved for the large-scale warming which happens every few years. The opposite phase—unusually cold SSTs in the eastern equatorial Pacific—is often now referred to as *La Niña*.

[4] 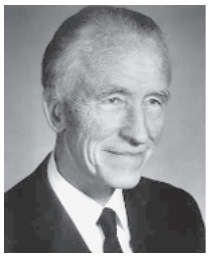

Jacob Bjerknes (1897–1975), Norwegian-American meteorologist and Professor at UCLA; son of Vilhelm Bjerknes, the Norwegian pioneer of modern meteorology. Jacob was the first to realize that the interaction between the ocean and atmosphere could have a major impact on the circulation of the atmosphere. He described the phenomenon that we now know as El Niño.

equation of motion is, from Eq. 10-3, anticipating a weak circulation and so neglecting nonlinear advective terms and replacing f by βy:

$$-\beta y v = \frac{1}{\rho_{ref}}\left(-\frac{\partial p}{\partial x} + \frac{\partial \tau_x}{\partial z}\right). \qquad (12\text{-}3)$$

Now, since the wind stress is assumed independent of x, we look for solutions such that all variables are also independent of x, in which case the pressure gradient term in Eq. 12-3 vanishes, leaving

$$-\beta y v = \frac{1}{\rho_{ref}}\frac{\partial \tau_x}{\partial z}\ .$$

If the deep ocean is quiescent, τ must vanish below the mixed layer; so the above equation can be integrated across the mixed layer to give

$$-\beta y \int_{-h}^{0} v\, dz = \frac{\tau_{wind_x}}{\rho_{ref}}\ , \qquad (12\text{-}4)$$

which simply states that the Coriolis force acting on the depth-integrated mixed layer flow is balanced by the zonal component of the wind stress τ_{wind}.

In response to the westward wind stress ($\tau < 0$) associated with the easterly tropical trade winds, the flow above the thermocline will be driven northward north of the equator ($y > 0$), and southward for $y < 0$; there is therefore divergence of the flow and consequent upwelling near the equator, as shown in Fig. 12.5. In fact, most of this upwelling is confined to within a few degrees of the equator. In the extratropics, we saw that the adjustment between the mass field and the velocity field in a rotating fluid sets a natural length scale, the deformation radius, $L = \sqrt{g'h}/f$, where

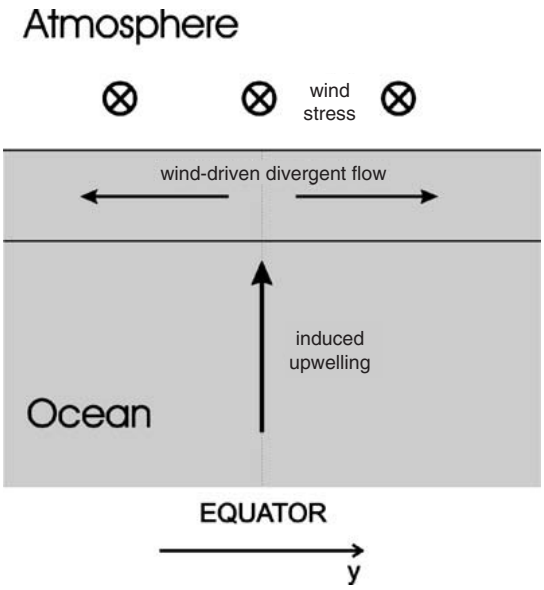

FIGURE 12.5. Schematic meridional cross section of the near-equatorial upwelling induced by a westward wind stress near the equator. Since the upper-layer flow is divergent, mass continuity demands upwelling through the thermocline.

we have replaced 2Ω by f in Eq. 7-23 of Section 7.3.4 and $g' = g(\rho_1 - \rho_2)/\rho_1$ is the reduced gravity. Here, near the equator, f is no longer approximately constant; for motions of length scale L centered on the equator, $f \sim \beta L$ and so $L^2 \simeq g'h/\beta^2 L^2$, thus defining the *equatorial deformation radius*

$$L_e = \left(\frac{g'h}{\beta^2}\right)^{1/4}.$$

For typical tropical ocean values $h = 100$ m, $g' = 2 \times 10^{-2}$ m s^{-2}, the above gives $L_e \sim$ 250 km, or about 2.25° of latitude. This is the natural length scale (in the north-south direction) for oceanic motions near the equator.[5]

This upwelling brings cold water up from depth, and thereby cools the upper layers of the near-equatorial ocean. We have in fact

[5]Eq. 12-4 is not valid within a distance of order $Y \sim L_e$ of the equator, but this does not affect our deductions about upwelling, since the continuity equation can simply be integrated in y across this region to give, at the base of the mixed layer, $\int_{-Y}^{Y} w\, dy = h\,[v(Y) - v(-Y)]$, yielding the same integrated result without needing to know the detailed variations of $v(y)$ between $\pm Y$.

already seen evidence for this upwelling in the thermal structure: the meridional cross-sections of T in Figs. 9.5 and 9.9 of Chapter 9 show clear upward displacement of the temperature contours near the equator. It shows even more clearly in the distribution of tracers, such as dissolved oxygen, shown in Fig. 11.14.

In reality, of course, the tropical Pacific Ocean is bounded to the east (by South America) and west (by the shallow seas in the region of Indonesia), unlike as assumed in the preceding calculation. One effect of this, in addition to the response to the westward wind stress deduced above, is to make the thermocline deeper in the west, and shallower in the east, as depicted in Fig. 12.6. In consequence, the cold deep water upwells close to the surface in the east, thus cooling the sea surface temperature (SST) there. In the west, by contrast, cold water from depth does not reach the surface, which consequently becomes very warm. This distribution is evident in the equatorial Pacific and (to a lesser degree) Atlantic Oceans (Fig. 9.3). A closeup view of Pacific SST distributions during a warm year (1998) and a cold year (1989) are shown in Fig. 12.7. Note the ''cold tongue'' in the cold year 1989 extending along the equator from the South American coast. Its narrowness in the north-south direction is a reflection of the size of the equatorial deformation radius. Aside from being cold, deep ocean water is also rich in inorganic nutrients; thus, the upwelling in the east enriches the surface waters, sustaining the food chain and a usually productive fishery off the South American coast.

The east-west gradient of SST produced by the wind stress in turn influences the atmosphere. The free atmosphere cannot sustain significant horizontal gradients of temperature, because for a finite vertical wind shear, thermal wind balance, Eq. 7-24, demands that $\nabla T \to 0$ as $f \to 0$ at the equator. The regions most unstable to convection are those with the warmest surface temperature. So convection and hence rainfall occurs mostly over the warmest water, which is over the ''warm pool'' in the western equatorial Pacific, as depicted in Fig. 12.6. The associated latent heating of the air supports net upwelling over this region, which is closed by westerly flow aloft, descent over the cooler water to the east, and a low-level easterly return flow. This east-west overturning circulation is known as the ''Walker circulation''. While here we have considered this circulation in isolation, in reality it coexists with the north-south Hadley circulation (discussed in Chapter 8). In association

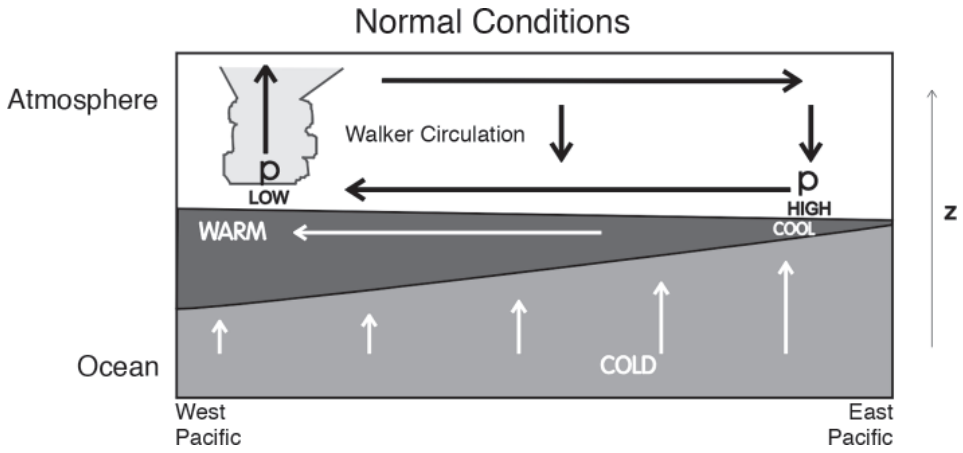

FIGURE 12.6. Schematic E-W cross section of ''normal'' conditions in the atmosphere and ocean of the equatorial Pacific basin. The east-west overturning circulation in the atmosphere is called the Walker Circulation.

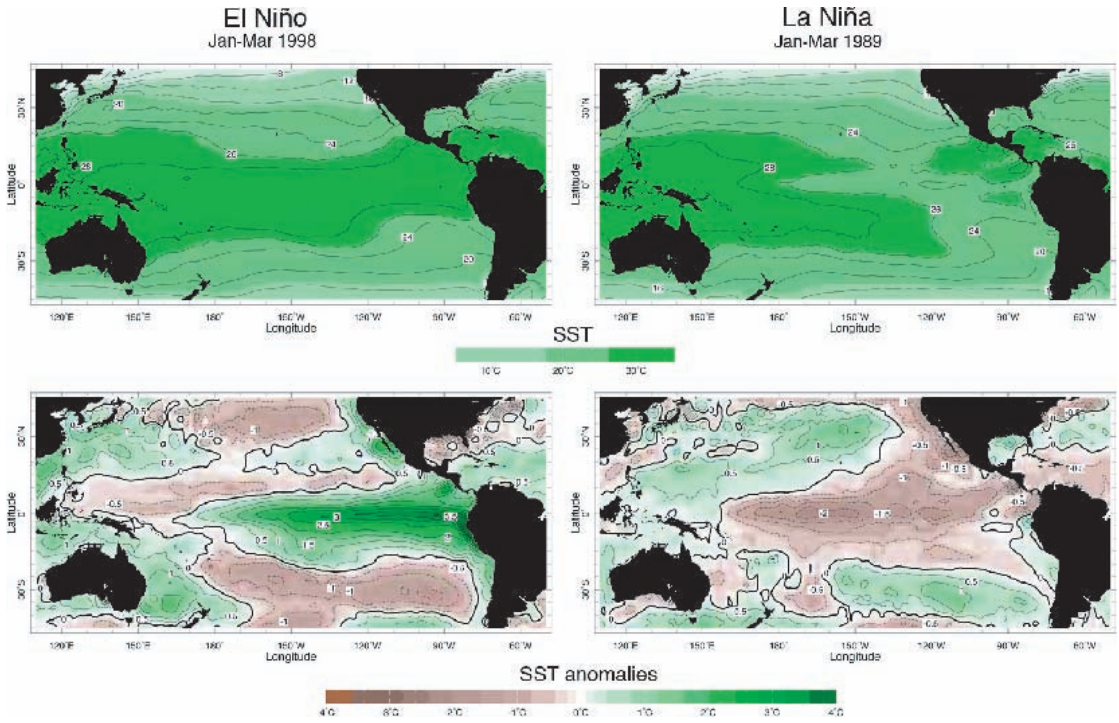

FIGURE 12.7. Sea surface temperatures (SST) (top) and SST anomalies (departure from long-term Jan-Mar mean; bottom) during an El Niño (warm event; left) and La Niña (cold event; right). Green represents warm anomalies, brown cold. Courtesy of NOAA.

with the circulation, there is an east-west equatorial gradient of surface pressure, with low pressure in the west (where the convection occurs) and higher pressure in the east (see Fig. 7.27).

Note that the low-level easterly flow present in the Walker circulation reinforces the trade winds over the equatorial Pacific. In fact, the causal links that were discussed previously can be summarized as in Fig. 12.8. There is thus the potential for positive feedback in the Pacific Ocean-atmosphere system, and it is this kind of feedback that underlies the variability of the tropical Pacific.

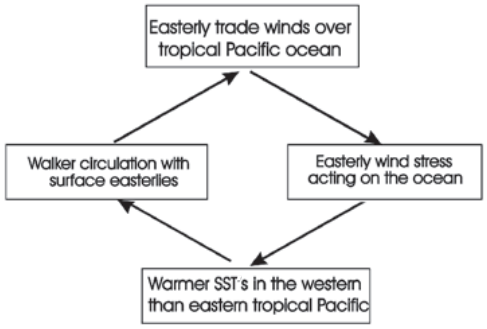

FIGURE 12.8. Schematic of the feedback inherent in the Pacific Ocean-atmosphere interaction. This has become known as the *Bjerknes feedback*.

12.2.3. ENSO

Atmospheric variability: The Southern Oscillation

As Walker noted, the Southern Oscillation shows up very clearly as a ''see-saw'' in sea level pressure (SLP) across the tropical Pacific basin. When SLP is higher than normal in the western tropical Pacific region, it tends to be low in the east, and vice versa. This can be made evident by showing how SLP at one location is related to that elsewhere.

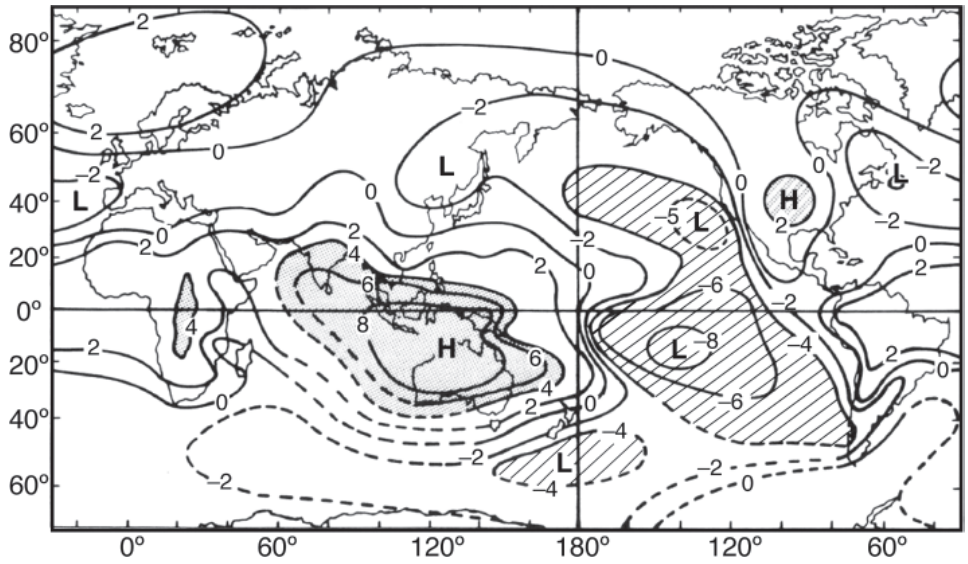

FIGURE 12.9. Correlations (×10) of the annual-mean sea level pressure with that of Darwin (north of Australia). The magnitude of the correlation exceeds 0.4 in the shaded regions. After Trenberth and Shea (1987).

Fig. 12.9 shows the spatial structure of the temporal correlation[6] of annual-mean SLP with that of Darwin (northern Australia). The correlation reveals a trans-Pacific dipole, with structure roughly similar to that of the Walker cell. Because of the location of the cell that anticorrelates with Darwin SLP, Tahiti SLP is frequently taken to be representative of this cell. It has become conventional to define a ''Southern Oscillation Index'' (SOI) as

$$SOI = 10 \times \frac{SLP_{Tahiti} - SLP_{Darwin}}{\sigma},$$

where σ is the standard deviation of the pressure difference. The time series of this index for the period 1951–2000 is shown by the solid curve in Fig. 12.10.

The index shows persistent but irregular fluctuations on periods of 2–7 years, with a few outstanding events, such as 1982–1983 and 1997–1998. Since, by definition, $SOI = 0$ under normal conditions—if by ''normal'' we mean the long-term average—Fig. 12.10 makes it clear that the tropical atmosphere is rarely in such a state, but rather fluctuates around it.

Such SLP variability is indicative of variability in the meteorology of the region as a whole as well as (to a lesser degree) of higher latitudes. Note, for example, the hint of an impact outside the tropics (such as the L-H-L pattern across N. America) in Fig. 12.9.

Oceanic variability: El Niño and La Niña

Figure 12.10 also shows (dashed curve) a time series of SST anomalies (departures from normal for the time of year) in the far eastern equatorial Pacific Ocean. Like the SOI, the SST shows clear interannual fluctuations on a typical time scale of a few years, and shows a dramatic anticorrelation with the SOI. The correlation coefficient between the two time series, over the period shown, is $C = -0.66$. The negative sign of the correlation, together with the spatial pattern of

[6]If two time series are perfectly correlated, then the correlation $C = +1$; if perfectly anticorrelated $C = -1$. If they are uncorrelated, $C = 0$.

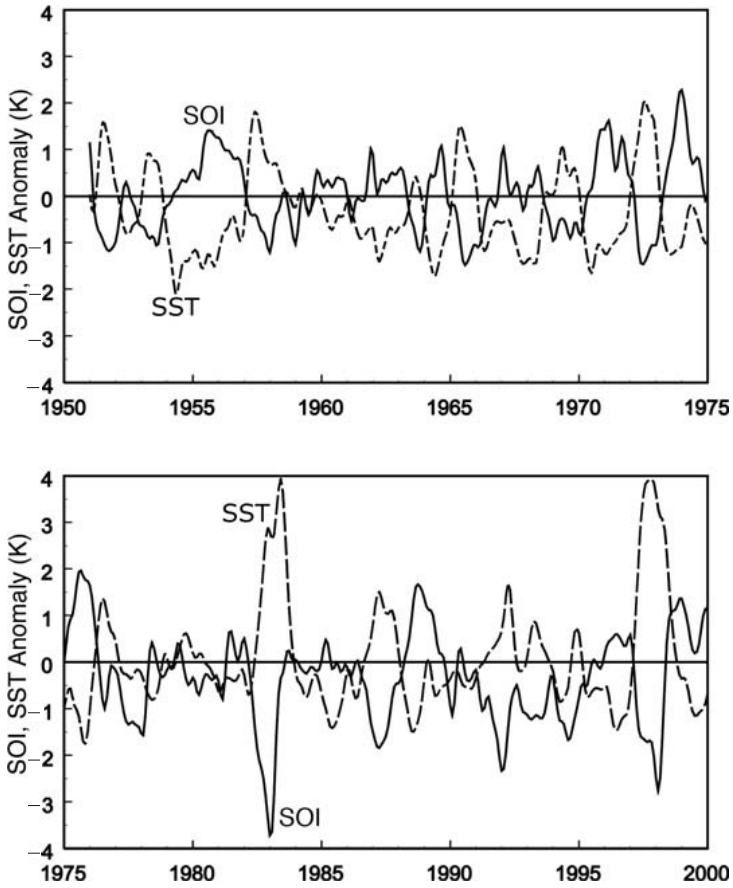

FIGURE 12.10. The Southern Oscillation index (solid) and sea surface temperature (SST) anomaly (K) in the equatorial east Pacific Ocean (dashed), for the period 1951–2000. The SST anomaly refers to a small near-equatorial region off the coast of South America. The two time series have been filtered to remove fluctuations of less than about 3 months.

Fig. 12.9, tells us that warm SST in the east equatorial Pacific approximately coincides with anomalously high pressure in the west and low in the east.

The spatial structure of SST variations is revealed by comparison of the two cases shown in Fig. 12.7. As noted previously, during ''normal'' or cold conditions, when the SSTs in the eastern equatorial Pacific are at their coldest (illustrated by the case of 1989), the coldest tropical water is concentrated in a narrow tongue extending outward from the South American coast, while the warmest water is found in an extensive warm pool west of the International Date Line. During a warm El Niño event (illustrated by the case of 1998), the warm water extends much further eastward, and the cold tongue is anomalously weak (in a strong event it may disappear). At such times, the eastern ocean, though still no warmer than the western equatorial Pacific waters, is very much warmer than normal for that time of year. While most of the equatorial Pacific Ocean is anomalously warm, the SST *anomalies* are greatest in the east, where they can be as large as 5 °C. Note from Fig. 12.7 that, for the most part, significant SST variability is concentrated within a few degrees latitude of the equator, consistent with our earlier estimate of the equatorial deformation radius.

Theory of ENSO

The ''big picture'' of what happens during a warm ENSO event is illustrated schematically in Fig. 12.11. As discussed above, in cold conditions, there is a strong east-west tilt of the thermocline and a corresponding east-west gradient of SST, with cold upwelled water to the east and warm water to the west. Atmospheric convection over the warm water drives the Walker circulation, reinforcing the easterly trade winds over the equatorial ocean. During a warm El Niño event, the warm pool spreads eastward, associated with a relaxation of the tilt of the thermocline. Atmospheric convection also shifts east, moving the atmospheric circulation pattern with it. Pressure increases in the west and decreases in midocean. This adjustment of the Walker circulation, which corresponds to a negative SOI, leads to a weakening or, in a strong event, a collapse of the easterly trade winds, at least in the western part of the ocean. We can summarize the mutual interaction as follows.

First, *the atmosphere responds to the ocean: the atmospheric fluctuations manifested as the Southern Oscillation are mostly an atmospheric response to the changed lower boundary conditions associated with El Niño SST fluctuations.* We should expect (on the basis of our previous discussion) that the Walker circulation and its associated east-west pressure gradient, would be reduced, and the Pacific trade winds weakened, if the east-west contrast in SST is reduced as it is during El Niño. There have been many studies using sophisticated atmospheric general circulation models (GCMs) that have quite successfully reproduced the Southern Oscillation, given the SST evolution as input.

Second, *the ocean responds to the atmosphere: the oceanic fluctuations manifested as El Niño seem to be an oceanic response to the changed wind stress distribution associated with the Southern Oscillation.* This was first argued by Bjerknes, who suggested that the collapse of the trade winds in the west Pacific in the early stages of El Niño (see the lower frame of Fig. 12.11) drives the ocean surface waters

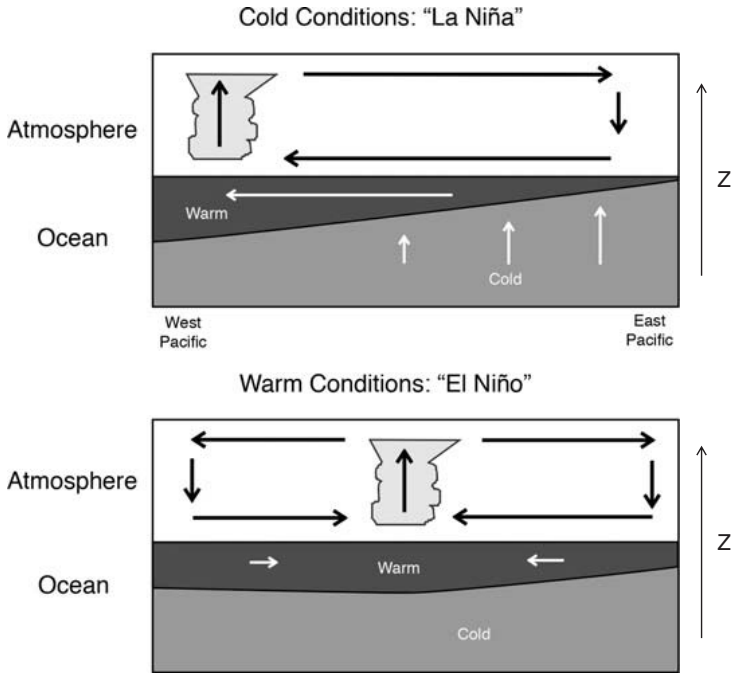

FIGURE 12.11. Schematic of the Pacific Ocean-Atmosphere system during (top) cold La Niña and (bottom) warm El Niño conditions.

eastward (through eastward propagation of a wave of depression on the thermocline); this deepens the thermocline in the east Pacific some two months later. This in turn raises the SST in the east. The basic postulate—that the ocean responds to the atmosphere—has been confirmed in sophisticated ocean models forced by ''observed'' wind stresses during an El Niño event.

Third, *the El Niño-Southern Oscillation phenomenon arises spontaneously as an oscillation of the coupled ocean-atmosphere system.*Bjerknes first suggested that what we now call ENSO is a single phenomenon and a manifestation of ocean-atmosphere coupling. The results noted previously appear to confirm that the phenomenon depends crucially on feedback between ocean and atmosphere. This is demonstrated in coupled ocean-atmosphere models of varying degrees of complexity, in which ENSO-like fluctuations may arise spontaneously. It appears that stochastic forcing of the system by middle latitude weather systems, which can reach down into the tropics to induce ''westerly wind bursts,'' can also play a role in triggering ENSO events.

Once the El Niño event is fully developed, negative feedbacks begin to dominate the Bjerknes positive feedback, lowering the SST and bringing the event to its end after several months. The details of these negative feedbacks involve some very interesting ocean dynamics. In essence, when the easterlies above the central Pacific start weakening at the beginning of the event, it leads to the formation of an off-equatorial shallower-than-normal thermocline signal, which propagates westward, reflects off the western boundary of the Pacific, and then travels eastwards. After a few months delay the thermocline undulation arrives at the eastern boundary, causing the thermocline to shoal there, so terminating the warm event.

12.2.4. Other modes of variability

The ENSO phenomenon discussed previously is a direct manifestation of strong coupling between the tropical atmosphere and tropical ocean and it gives rise to coherent variability in the coupled climate. There are other modes of variability that arise internally to the atmosphere (i.e., would be present even in the absence of coupling to the ocean below). Perhaps the most important of these is the *annular mode*, a meridional wobble of the subtropical jet stream. The climatological position of the zonal-average, zonal wind, $\overline{u}$, is plotted in Fig. 5.20. But in fact the position and strength of the jet stream maximum varies on all timescales; when it is poleward of its climatological position, $\overline{u}$ is a few $\mathrm{m\,s^{-1}}$ stronger than when it is equatorward. These variations in $\overline{u}$ extend through the depth of the troposphere and indeed right up into the stratosphere. Importantly for the ocean below, the surface winds and air-sea fluxes also vary in synchrony with the annular mode, driving variations in SST and circulation. The manifestation of the annular mode in the northern hemisphere, is known as the *North Atlantic Oscillation*, or NAO for short; the annular mode in the southern hemisphere is known as SAM, for *southern annular mode*. Both introduce stochastic noise into the climate system that can be reddened by interaction with the ocean as discussed in Section 12.1.1.

12.3. PALEOCLIMATE

Here we briefly review something of what is known about the evolution of climate over Earth history. Fig. 12.12 lists standard terminology for key periods of geologic time. Study of paleoclimate is an extremely exciting area of research, a fascinating detective story in which scientists study evidence of past climates recorded in ocean and lake sediments, glaciers and icesheets, and continental deposits. Proxies of past climates are myriad, and to the uninitiated at least, can be bizarre (packrat middens, midges...), including such measurements as the isotopic ratios of shells buried in ocean sediments, thickness and